Proceedings of the ASME Pressure Vessels & Piping Division / K-PVP Conference
PVP2010
July 18-22, 2010, Bellevue, Washington, USA

PVP2010-25823

EXPERIMENTAL AND CFD EVALUATION OF A BUBBLE COLUMN REACTOR

Sean M. McGuffie
Porter McGuffie, Inc.
Lawrence, KS, USA
785-856-7575 x102
sean@pm-engr.com

Mike A. Porter
Dynamic Analysis
Lawrence, KS, USA
785-843-3558
mike@dynamicanalysis.com

Dennis H. Martens
Porter McGuffie, Inc.
Lawrence, KS, USA
913-484-3868
martensdh@pm-engr.com

ABSTRACT

During the scale-up design of a slurry bubble column reactor from a pilot demonstration facility to a production reactor, the design team used computational fluid dynamics (CFD) as a tool to quantify design variables, such as gas holdup and liquid velocities/structural pressures within the reactor. At the time of the analysis, all available physics models for modeling the multi-phase flow had significant limitations that would require "tuning" of the CFD input parameters to ensure confidence in the results. The authors initially conducted a literature search to find data that could be used to calibrate the model. While a wide variety of literature is available, none provided the exact data required for model calibration. For this reason, the authors constructed a test column and performed experiments to derive data for tuning the CFD models. Statistical analysis of the experimental data provided distributions on the input parameters of interest. CFD studies were then used to tune the CFD input parameters to match the experimental data. A correlation was developed, tested and verified. This correlation was then used to provide confidence in the results of the design analysis performed on the scaled up reactor.

INTRODUCTION

A bubble column reactor (BCR) consists of a vessel, typically filled with a multi-phase mixture. The mixture often consists of a liquid reactant phase; a gas reactant phase injected at the bottom of the vessel through a sparger; and in some cases solid, dispersed catalyst particles. This paper examines a special case known as a slurry bubble column reactor (SBCR). The buoyancy of the gas bubbles causes them to rise through the liquid. During the bubbles' rise, they contact the liquid and the dispersed catalyst particles leading to chemical reactions and the generation of a product species.

Bubble column reactors are used in a wide variety of chemical processes involving reactions such as oxidation, chlorination, alkylation, polymerization and hydrogenation. The diversity of applications rises from both the reaction and design advantages that they provide. For reactions, they provide excellent heat and mass transfer characteristics. In design and operation, they provide a low maintenance reactor vessel with few moving parts and, typically, the ability to cycle catalysts while in operation (Kantarci [1]).

The conversion efficiency of the SBCR is dependent on several parameters, including the contact time of the bubbles with the fluid, contact surface area of the bubbles, the amount of dispersed catalyst contacted, and the total gas hold-up within the column. Therefore, prudent design considers factors such as bubble spatial and size distribution from the injection sparger and typical fluid flow patterns through the reactor. Additionally, the design of reactors typically involves consideration of the pressures exerted on the vessels' internal components due to fluid-structure interaction (Krishna [2]).

NOMENCLATURE

Holdup	=	The amount of gas present in the column or vessel
Volume Fraction	=	Fraction of gas in an individual cell within the CFD model
Sγ	=	Methodology used in CD-Adapco's

		Extended Framework to calculate coalescence and break-up
SV	=	Superficial velocity – Volumetric flow rate of gas / cross sectional area of vessel
Y+	=	u*y/ν, used in defining the law of the wall
u*	=	Friction velocity
y	=	Distance to nearest wall
ν	=	Local kinematic viscosity
k-ε	=	Two-equation Reynold's averaged Navier Stokes (RANS) turbulence model

PROBLEM DESCRIPTION

The authors were tasked with performing computational fluid dynamics (CFD) analyses on a vessel under design. The primary task of the analyses was to provide numerical values for the aforementioned quantities for verification of the fluid dynamics design of the vessel and for input into structural analysis models.

Full consideration of the problem would require a CFD model that considered all 3 species and the chemical reaction generating a product. It was determined through consultation with the design team that the reactions would not be considered and that due to its low volume fraction, the dispersed catalyst phase would be considered through a modification to the fluid's viscosity, resulting in simplified analyses.

Due to internal considerations, as well as the robustness of physics models offered, Star-CD from CD-Adapco was chosen to perform the analyses. The literature search performed before the analyses indicated that a range of bubble sizes between 9 and 22 mm (0.35 and 0.87 in) should be expected with bubble breakup and coalescence occurring as the bubble travels through the reactor. Additionally, gas holdups between 15 and 40% could be expected (Koide [3], Schafer [4]). At the time of the analyses, Star-CD offered four options for modeling the 2-phase flow problem: volume of fluid (VOF), Lagrangian 2-phase, Eulerian 2-phase (E2P), and E2P with the Extended Framework.

AVAILABLE PHYSICS MODEL DESCRIPTIONS

The VOF model explicitly calculates the interaction of the two phases with the assumption that they are immiscible. Breakup and coalescence are modeled through consideration of the bubble pressure due to fluid forces and/or bubble collisions and the surface tension of the bubble within the fluid. Proper spatial resolution of the bubbles or secondary dispersed phase requires at least 3 computational cells across each outer surface of the bubble (CD-Adapco [5]). Additionally, solution of the VOF model is inherently transient, requiring a large number of solution time-steps to reach steady-state. As the subject vessel had a volume greater than 2000 m^3 (100 x 10^6 in^3), proper spatial resolution of the bubbles would require more than 50 billion cells, an unreasonable model size.

The Lagrangian 2-phase model is generally limited to dispersed phase volume fractions of less than 10%. As the expected gas holdup within the reactor was at least 25%, this model was not applicable to the problem under consideration.

The E2P model treats the phases as interpenetrating continua. Separate equations for each phase's momentum and energy are solved with transfers of these quantities tracked through inter-phase transfer terms. Volume fractions for each phase are calculated on a cell-by-cell basis and are reported during the solution. Additionally, the fluid properties for the cell are modified based on the calculated volume fraction. The E2P model also allows for a quasi-steady state solution. Using this procedure, an initial flow field is calculated for the continuous phase. Next, a series of iterative analyses are performed to calculate the initial trajectories of the dispersed phase and the inter-phase transfer terms. The continuous phase solution is then updated. This iterative procedure is continued until acceptable convergence has been achieved. As there is not explicit time integration of the solution, significant amounts of computer resources are conserved (CD-Adapco [6]). It should be noted that the quasi-steady-state solution of the E2P model only provides a probabilistic distribution of velocities within the vessel, so no time component can be calculated.

The E2P model with the Extended Framework uses the Sγ approximation to account for the breakup and coalescence of bubbles due to several complex models (Lo [7]). There were a number of parameters that required experimental data to determine their values. Additionally, the values of these parameters can significantly affect the calculated flow patterns and bubble size distributions. Consequently, it was determined that the E2P with Extended Framework model could not be used to provide design data with an acceptable level of confidence.

As can be seen from the physics model descriptions above there was only one model that was deemed suitable, gauged through the ability to provide design information with confidence for the problem under consideration, the standard E2P model.

SPECIFIC PROBLEM DESCRIPTION

At the time of the analysis, the implementation of the E2P model allowed for only the consideration of a single bubble diameter for the dispersed phase. It had previously been shown that a distribution of bubble sizes should be expected within the column. Therefore, it was necessary to establish an acceptable bubble diameter for use in the analyses. For this reason, the authors decided to conduct experimental analyses on a small bubble column to determine gas holdup and expected bubble diameters. The experiments performed with the bubble column apparatus would be captured using digital video. Routines using image analysis software and statistical analysis packages would be used to characterize the bubbles and gas holdup within the columns.

Next a CFD model was constructed of the column and a series of analyses were then used to "tune" the bubble diameter

based on experimental inputs so that an acceptable level of correlation was achieved with the results. These tuned bubble diameters were then used to determine if a correlation could be developed to allow extrapolation of the data to more situations.

INITIAL EXPERIMENTAL DETERMINATION OF BUBBLE SIZE

To perform the experiments, a water-air bubble column was constructed. The column consisted of a clear polycarbonate cylinder with an ID of 5.75 in (146 mm) with a sparger located 1" (25.4 mm) above the bottom. The column was supported with a wood stand with periodic levels to provide vertical support. An image of the column is contained in Figure 1.

Air was supplied to the column through the use of a 3 Hp air compressor. A volumetric flow gauge was then placed inline between the compressor and the column's sparger. The volumetric flow rate to the column was varied using the compressor's pressure regulator to vary superficial velocity. For reasons discussed in the CFD Analysis section, two different sparger designs were used during experimentation: an open top wire mesh sparger and a closed top, bottom exit sparger. Figure 2 shows the two spargers used during the experiments.

The results of each experiment were captured using a digital camera focused on the free surface of the water in the column. The camera captured color images at a resolution of 640 x 480 pixels and 15 frames per second. Two black stripes were placed on the column to allow calibration of distances within each frame analyzed. A halogen light was used to illuminate the front of the column and a white background was provided to increase contrast on the captured video.

The video files, captured as AVIs, were separated into individual bitmap images. A custom MatLab [8] routine was developed to analyze each image. To perform the analysis, the following steps were taken:

Calibration of measurement environment – a series of representative images from the video capture were scanned to determine the top and bottom of the measurement area, as well as the horizontal limits of the area.

Conversion to grayscale – All images from the video capture were converted to grayscale to increase contrast for determining the extents of the free surface. A grayscale color limit was then manually determined from a series of frames to establish the interface between the water and air. The calibration of the color limit accounted for variations in the test environment lighting.

Data mining – Each frame was mined by scanning from top to bottom to determine the peak height of the free surface, as well as the shape of the free surface above the starting water height. The area of the shape of the free surface, projected to a 2-dimensional plane was then integrated to find the average height of the free surface. Figure 3 shows a frame capture of the complete apparatus and a capture as processed by the data mining routine.

Data analysis – Routines were implemented in the data mining routine to perform analyses on the extracted data, including FFT analyses of the free surface average and maximum heights and statistical analyses of the data. More description on the routines and their utilization is provided in the Bubble Size Analysis section below.

The experiments were performed several times at varying superficial velocities to establish trends within the data. The superficial velocities considered during experimentation were 0.08 m/s, 0.16 m/s, 0.24 m/s and 0.32 m/s (3.15 in/s, 6.3 in/s, 9.5 in/s and 12.6 in/s).

Several experiments were performed to quantify the amount of variance introduced into the experimental data due to the test setup. These tests included changing the sparger type and varying the initial column-starting height. The results of these experiments are also presented below.

BUBBLE SIZE ANALYSIS

The average gas holdup in the column was derived from the average height of the free surface during the experiment. The MatLab routine also calculated the standard error for the measured volume fractions at each superficial velocity. Figure 4 shows the results of the series of experiments performed with the column.

The next step in deriving the bubble size from the experiments was to perform an FFT on the difference in height between the peak surface level and the average surface height. The FFT would provide an indication of the number of bubbles that were being released to the atmosphere over a period of time. The frequency content from the experimental data should also provide an indication of the distribution of bubbles leaving the free surface, as small bubbles would be expected to depart at a higher frequency than large bubbles. Figure 5 shows representative FFTs from the experiments.

The FFT data showed that the frequency content for each superficial velocity was different, but the frequency content for a specific superficial velocity was comparable. It was observed during experimentation that larger bubbles existed at higher superficial velocities. Thus, the shift in peaks versus superficial velocity also confirmed the theory on bubble size distribution.

It was also theorized that a greater difference between peak and average water levels would be indicative of larger bubble sizes. To analyze whether this was the case, quantile-quantile plots were created using the *qqplot* function in the MatLab Statistics Toolbox [9]. A quantile-quantile plot compares the probability distribution functions of two series to determine if they come from the same distribution. It is generally accepted that if the series are from the same distribution, the data points will fall on a straight line (NIST [10]). Figure 6 shows sample quantile-quantile plots from the experiments. As can be seen from the plots in Figure 6, the series data fall along a reasonably straight line. For this reason it can be concluded that for each superficial velocity the bubble sizes come from the same distribution.

To qualify the type of distribution that best characterized the data, histograms were developed of the height differential evidenced during the experiments. Fits were then performed on the histogram data using Weibull, Gamma and Lognormal distributions. These distributions were chosen due to the shape of the histograms. Figure 7 shows a sample fit on a set of experimental data. As can be seen from the histogram plot in Figure 7, the Lognormal distribution best fits the histogram data from the experiment.

The differential height data from all experiments were then fit using a Lognormal distribution to find the mean and standard deviations. Given a superficial velocity, or gas escape rate, a mean bubble diameter could then be determined from the assumed distributions by assuming that the mean and standard deviation of the bubble size was directly related to the mean of the water height fit. It was found that the means derived using this method differed by less than 1% at a given superficial velocity. Figure 8 shows the mean bubble diameters derived from the experiments using this methodology.

CFD ANALYSIS

A CFD model was developed of the bubble column. The model was constructed of hexahedral cells with boundary layer refinement performed at the walls so that the wall local Y+ value was less than 100. Two phases were defined for the analysis, water and air. Due to the short column depth, both phases were treated as incompressible. The E2P model was enabled with the air defined as the discrete phase. Due to limitations of the E2P model, only the k-ε turbulence model was used in the analyses. The standard drag law, as applicable for the bubble diameter under consideration, was used. For the initial analyses, the quasi-steady state analysis technique previously discussed was used. An initial volume fraction of 8% gas was defined to provide momentum sources for inter-phase transfer terms.

A series of analyses was performed for three of the four superficial velocities studied during experimentation: 0.16 m/s, 0.24 m/s, and 0.32 m/s. If a correlation could be derived from the CFD analyses, the 0.08 m/s superficial velocity case would be used to verify the correlation.

For the iterative analysis process, at each superficial velocity, the bubble diameter at the inlet was varied until the steady-state volume fraction in the CFD-modeled column was the same as the volume fraction obtained from experiments. Figure 9 shows the CFD-derived bubble sizes along with the data derived from experiments.

As can be seen from the curves in Figure 9, the fit performed on the CFD-derived values has a similar shape to the fit performed on the experimentally derived bubble size with an offset of approximately 0.42 in. The authors believe there are likely two causes for this offset: first, the use of the simple drag law does not represent the bubble drag over the entire population; and second, the methodology used to track the bubbles in the experimental processing converted a 3-dimensional free surface to a 2-dimensional plane for data analysis.

The fit shown in Figure 9 was then used to determine the bubble size required to achieve the correct holdup in the CFD model with a superficial velocity of 0.08 m/s. With the bubble size selected, an analysis was performed to determine the hold-up in the CFD model. This value was determined to be 15.86%, and the experimental holdup at this superficial velocity was 17%, indicating reasonable correlation.

While the fits derived from the CFD analyses were providing reasonable correlation, an attempt was made to determine why the offset between the experimental bubble sizes and the CFD derived bubble sizes existed. As a first step, the velocity results from the quasi-steady-state analyses were queried. A sample vertical velocity plot is shown in Figure 10.

A very high velocity value is seen just above the sparger in the Figure 10. It is computationally reasonable for this high velocity to exist in a region of high gas volume fraction, and therefore high buoyancy force. As previously mentioned, the quasi-steady-state analysis technique only provides a probabilistic view of the overall velocities within the column and therefore may underestimate the time variant forces acting on such a region. For this reason it was determined that a transient analysis using the more computationally intensive VOF model should be performed to quantify the time-varying shape of the high velocity region.

TRANSIENT ANALYSIS

To perform the transient analysis, the solution parameters were modified from the procedures outlined with the quasi-steady-state model above to include time integration of the bubble paths. Additionally, the initial volume fraction of the column was set to 0. This allowed complete development of the dispersed phase quantities along the same path from which the experimental results were derived. The analysis was performed for a long enough period of time so that the volume fraction in the column reached a steady-state value. The images in Figure 11 show the volume fraction predicted with the CFD analysis and the bubble distribution at comparable times after the start of gas flow.

As can be seen from Figure 11, the volume fraction distribution through most of the column is similar to the bubble distribution, with there being highly dispersed void areas in various sizes. Also evident in the image on the left in Figure 11 is a large area indicating a high volume fraction of bubbles directly over the sparger. As can be seen in the image on the right, the sparger tended to release a large bubble that immediately broke into many smaller bubbles that then travelled up the column. This caused a pulsing behavior at the sparger outlet during the experiment that was not replicated in the CFD model.

QUANTIFICATION OF POSSIBLE EXPERIMENT ERRORS

Due to the offset in bubble diameter determined during the CFD analysis and differences in the velocity and volume fraction patterns when the CFD results are compared to the experimental data, it was determined that steps should be taken to ensure that the data derived during the first experiments was not due to the experiment setup. To accomplish this, two parameters that were invariant during the original experiments - the sparger geometry and the initial height of the water in the cylinder - were varied in the test setup.

Due to the pulsation evident in the experiments, it was determined that the sparger geometry should be modified to change the injection characteristics into the cylinder. To accomplish this, the sparger was modified from the wire mesh sparger used in the original experiments to the bottom outlet sparger shown in Figure 2. Experiments were conducted at the previous superficial velocities to determine the effect of the sparger geometry on the gas holdup. Figure 12 shows the experimental holdups with the 2 sparger geometries. As demonstrated in the figure, there is no significant difference in the gas holdup based on the sparger geometry.

The second verification step that was performed with the experimental setup was to determine if the initial water height in the column affected the calculated results. To perform this verification step, the starting height of the column was set to 14.5 in and 24 in. Figure 13 shows the results of these experiments. As can be seen from the Figure, there are no significant differences caused by the column's initial water height.

CONCLUSIONS

A series of experiments were performed on a test bubble column to determine the parameters required for accurate analysis of bubble columns using the E2P model during CFD analysis. A correlation between the experimental and CFD models of the experimental apparatus was found and verified through the use of a separate CFD analysis. Additional experiments were performed to determine the influence on the sparger geometry and the initial column height on the experimental results. These experiments indicated that neither of these parameters significantly affected the experimental results. With verification of the correlation and independence of the experimental volume fraction on the test setup confirmed, the analysts were able to move forward with using the bubble sizing procedures for the design verification analysis. All design variables required from the CFD analysis of the vessel were provided to the client.

REFERENCES

[1] Kantarci, N., Borak, F., Ulgen, K.. 2005. Review – Bubble Column Reactors. *Process Biochemistry* 40 : 2263-2283.

[2] Krishna, R., van Baten, J. M., Urseanu, M. I. 2000. Three-phase Eulerian simulations of bubble column reactors operating in the churn-turbulent regime: a scale up strategy. *Chemical Engineering Science* 55 : 3275 – 3286.

[3] Koide, K., et. al. 1978. Behavior of Bubbles in Large Scale Bubble Column. *Journal of Chemical Engineering of Japan* : 98 -104.

[4] Schafer, R., Merten, C., Eigenberger, G. 2002. Bubble size distributions in bubble column reactor under industrial conditions. *Experimental Thermal and Fluid Science* 26 : 595 – 604.

[5] CD-Adapco, Star-CCM+ Users Guide, What is the VOF Multi-Phase Model, 2009

[6] CD-Adapco, Star-CD Methodology Guide, Chapter 13, 2005

[7] Lo, S. "Modeling Breakup and Coalescence using the S_γ model", CD-Adapco report, 2006

[8] MatLab, v. 7.5.0.342 (R2007b)

[9] MatLab Statistics Toolbox, v. 7.2 (2008)

[10] NIST/SEMATECH e-Handbook of Statistical Methods, http://www.itl.nist.gov/div898/handbook/

FIGURE 1 – EXPERIMENTAL TEST COLUMN

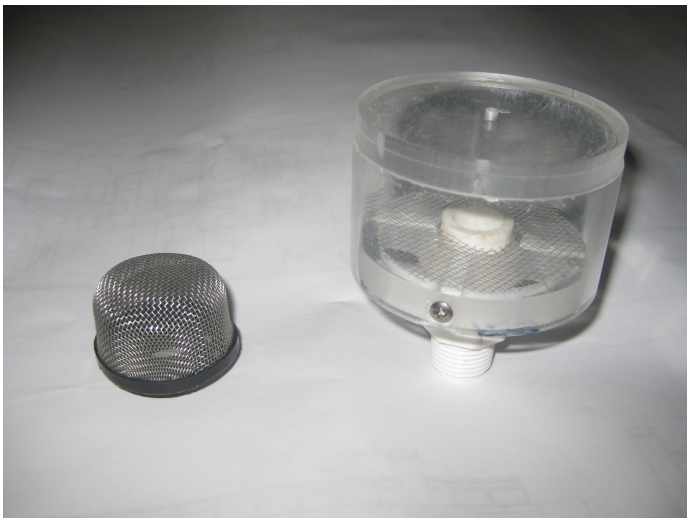

FIGURE 2 – SPARGERS USED DURING EXPERIMENTS

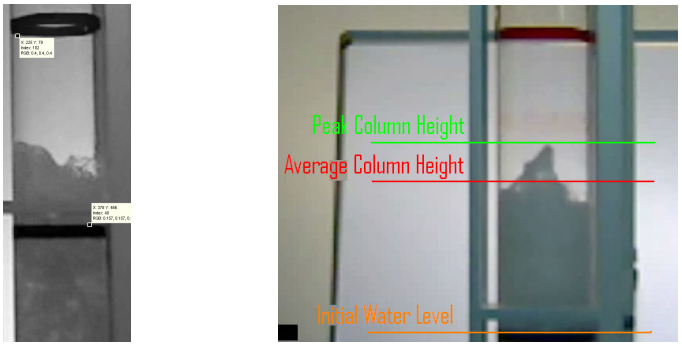

FIGURE 3 – CAPTURED AND PROCESSED IMAGES FROM EXPERIMENT

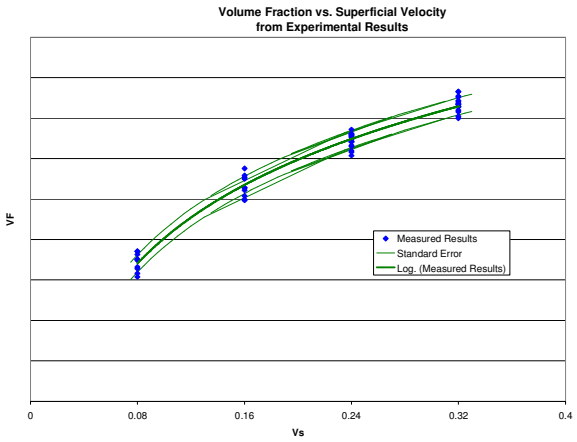

FIGURE 4 – EXPERIMENTALLY DERIVED VOLUME FRACTIONS

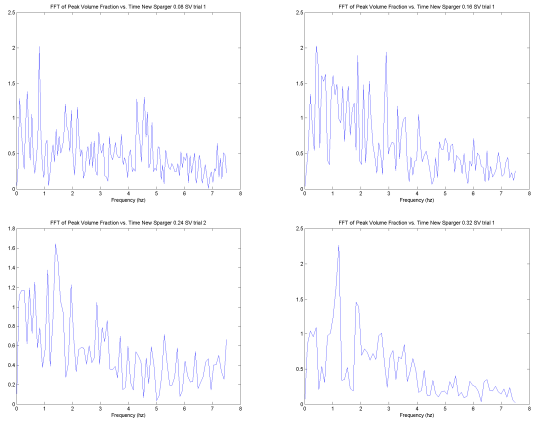

FIGURE 5 – REPRESENTATIVE FFTs OF EXPERIMENTAL DATA (0.08, 0.16, 0.24 and 0.32 m/s)

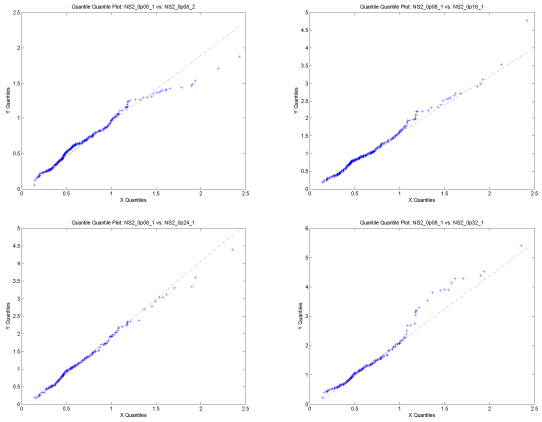

FIGURE 6 – SAMPLE QUANTILE-QUANTILE PLOTS FROM EXPERIMENTS

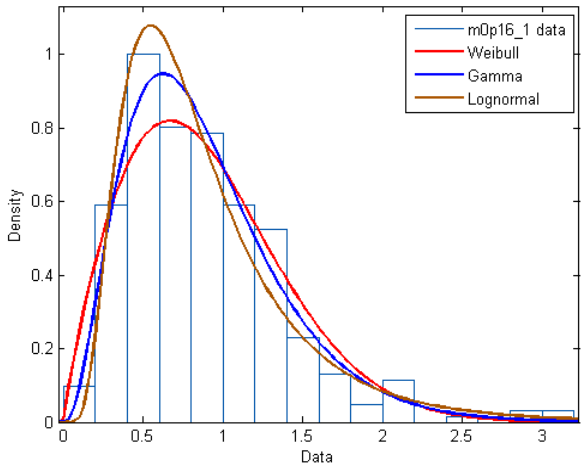

FIGURE 7 – HISTOGRAM DATA FROM 0.16 m/s SV EXPERIMENT

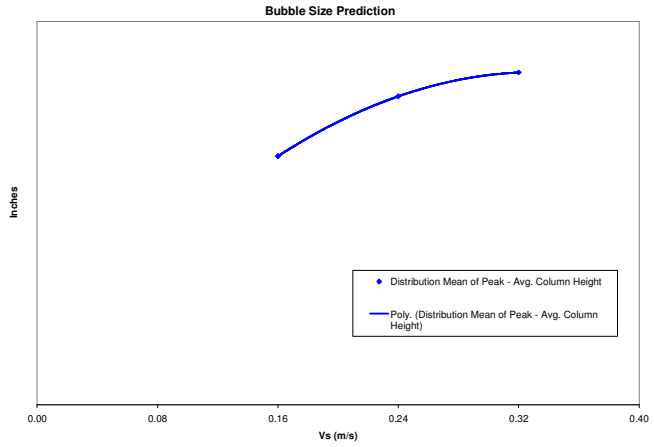

FIGURE 8 – PREDICTED BUBBLE SIZES FROM EXPERIMENTS USING LOGNORMAL DISTRIBUTION

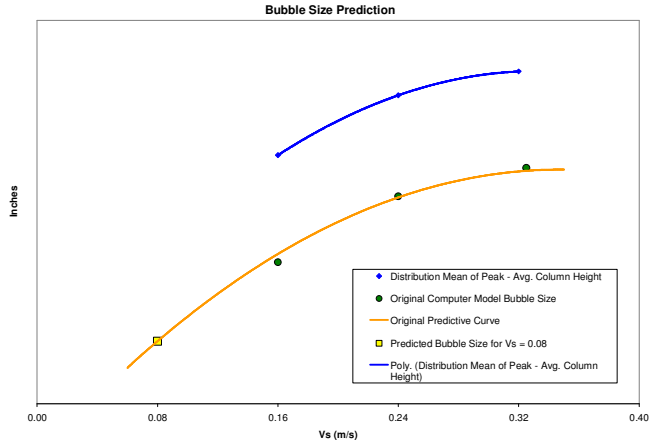

FIGURE 9 – CFD-PREDICTED BUBBLE DIAMETERS WITH EXPERIMENTALLY DERIVED VALUES

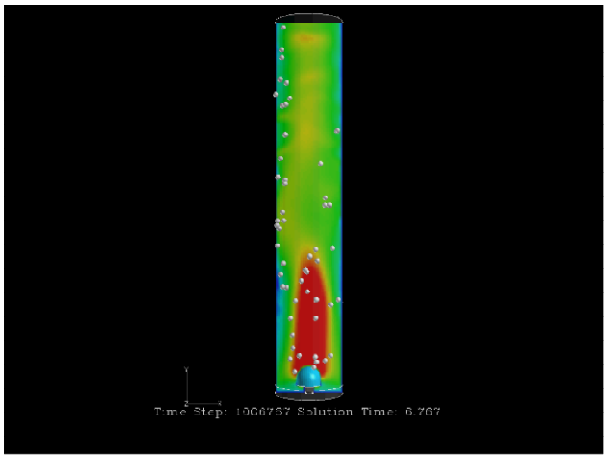

FIGURE 10 – SAMPLE VERTICAL VELOCITY PLOT FROM QUASI-STEADY-STATE ANALYSIS

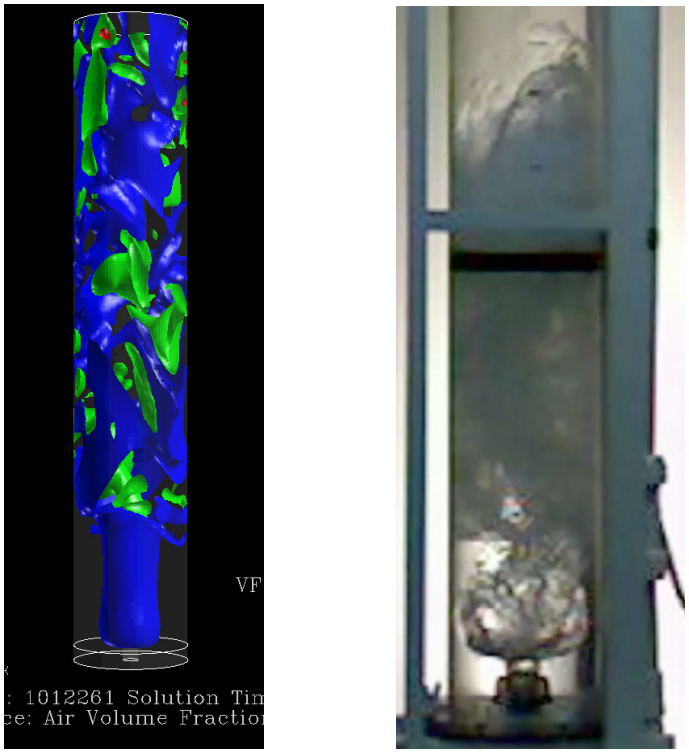

FIGURE 11 – COMPARISON OF CFD VOLUME FRACTION AND BUBBLE DISTRIBUTION

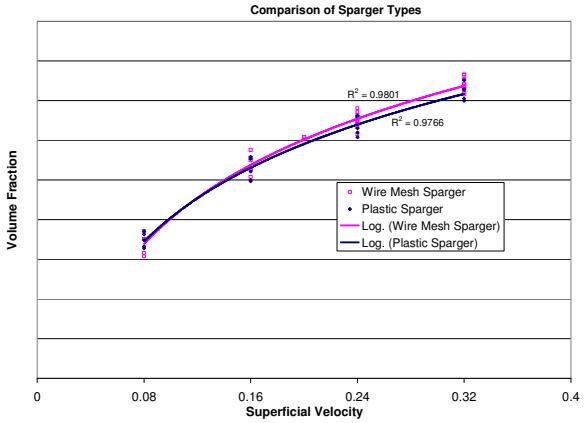

FIGURE 12 – COMPARISON OF SUPERFICIAL VELOCITY AND GAS HOLDUP FOR VARIOUS SPARGERS

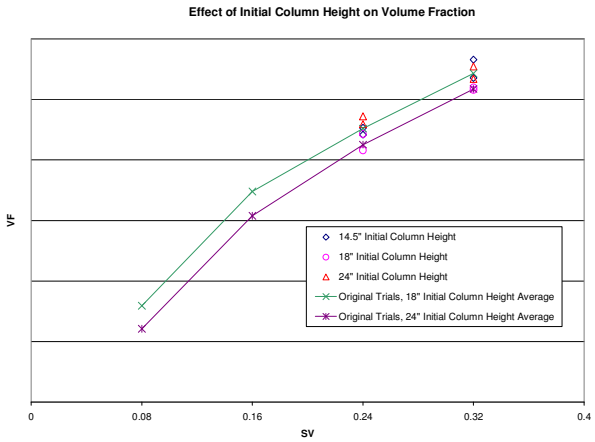

FIGURE 13 – COMPARISON OF VOLUME FRACTION WITH VARYING COLUMN HEIGHTS